ORIGINAL

Dissection of morphological and metabolic differentiation of ameloblasts via ectopic SP6 expression

Taro Muto, Keiko Miyoshi, Taigo Horiguchi, and Takafumi Noma

Department of Molecular Biology, Institute of Health Biosciences, the University of Tokushima Graduate School, Tokushima, Japan

Abstract : Tooth enamel is the hardest organ in the body. In rodent incisor, the enamel is exclusively produced by ameloblasts with yellowish-brown pigmentation, indicating normal enamel formation. However, the molecular mechanisms of ameloblast differentiation and amelogenesis are not fully understood. Specificity protein (Sp) 6 has been reported as one of the critical factors for tooth development. To explore SP6 function, we generated *Sp6* transgenic (Tg) rats. Unexpectedly, the enamel surfaces of the incisors in Tg rats were discolored, even though enamel formation and serum iron concentrations were normal. Histological analysis of incisors from 6-week-old Tg rats demonstrated that the ameloblast layer at the pigmentation stage was elongated up to the gingival margin with ectopic SP6 expression in longitudinal incisor sections. In contrast, the incisors from 10-week-old Tg rats revealed that the pigmented ameloblasts were morphologically changed to those of the reduced stage, concomitant with the sporadic disappearance of ectopic SP6 expression. Here we report that morphological differentiation and metabolism of the iron-containing pigment in ameloblasts are independently regulated during amelogenesis by means of ectopic SP6 expression. J. Med. Invest. 59 : 59-68, February, 2012

INTRODUCTION

Ameloblasts differentiate sequentially from the presecretory stage to the secretory and maturation stages to produce enamel (1). During these developmental stages, ameloblasts exhibit dramatic morphological changes, which are closely associated with their functions (1). In the case of rodents, the incisors grow continuously throughout their life. Ameloblasts covering the labial surface of the incisors migrate from the apical bud toward the incisal end and undergo morphological and functional differentiation simultaneously. Thereby, all stages of ameloblast differentiation are conveniently visible in the longitudinal sections at a glance (1).

The maturation stage of ameloblast differentiation is subdivided into six substages, namely postsecretory transition (rapidly decreasing ameloblast height), maturation proper (starting enamel maturation and development of the papillary layer), pigmentation (appearance of the pigment in the cytoplasm), pigment release (gradual disappearance of the pigment), postpigmentation (complete disappearance of the pigment), and reduced (marked reduction in the height and formation of a cuboidal shape) stages (1, 2). During these stages, ameloblasts metabolize the pigment, reduce their height gradually, and turn the color of the enamel surface to yellowish brown via unknown mechanisms (2-4). The ameloblast pigment is considered to be iron-containing ferritin which is transferred to lysosomes for degradation (1, 2, 5). Furthermore,

iron is metabolically processed in the ameloblasts and deposited on the enamel surface as a yellowish-brown layer (3, 4, 6).

Specificity protein (Sp) 6 belongs to the SP/KLF transcription factor family (7), and it plays important roles in tooth development and organogenesis of the limb buds, hair follicles, and lungs (8-10). *Sp6*-deficient mice show supernumerary teeth, enamel agenesis, defects in cusp and root formation, and abnormal dentin structure (9, 10). However, the molecular basis for the role of SP6 is not well understood. In this study, we generated *Sp6* transgenic (Tg) rats to investigate the roles of SP6 in tooth development. We found that incisor amelogenesis was perturbed in Tg rats, especially with regard to morphological differentiation and iron metabolism at late maturation stages, indicating that the stringent spacio-temporal control of *Sp6* gene expression is crucial for morphological differentiation and iron metabolism during amelogenesis.

MATERIALS AND METHODS

Sp6 Tg rats

Rat *Sp6* cDNA containing the coding region (1.1 kb) was cloned into the *Not*I sites in the multicloning sites of pCI-neo expression plasmid containing the human CMV immediate-early enhancer/promoter region (Promega, Madison, WI, USA) using the reverse transcription polymerase chain reaction (RT-PCR) as shown previously (11). A 2583-bp fragment containing the *Sp6* transgene components was prepared with *Bgl*II and *Cla*I digestion, and microinjected into fertilized eggs of Sprague-Dawley rats to obtain Tg rat founder lines (YS Institute, Tochigi, Japan). The Tg lines examined were maintained as hemizygotes by crossing them with WT SD rats for at least five generations. Progenies from the cross of male Tg and female WT rats were used for further analyses. Animal experiment was approved by the Ethics Committee for Animal Experiments of the University of Tokushima (No. 06105).

RT-PCR

Soft tissues and mandibular molars were obtained from 5-week-old rats and postnatal day 6 rats, respectively. Total RNA was isolated using the TRI reagent (MRC, Cincinnati, OH, USA) according to the manufacturer's instructions, and reverse transcribed with random 9-mers using the RNA PCR kit (AMV) version 3.0 (Takara Bio, Ohtsu, Japan). RT-PCR was performed using cDNA samples from Tg rats and their non-Tg littermates (WT) with GoTaq polymerase (Promega) and the following primers : pCI-neo.F (5'-GGC TAG AGT ACT TAA TAC GAC TCA C-3') and rSp6.R3 (5'-TCA TAG CCC TGT GAG AAG TC-3') for Tg *Sp6* amplification and GAPDH-S (5'-CAT TGA CCT CAA CTA CAT GG-3') and GAPDH-AS (5'-CTC AGT GTA GCC CAG GAT GC-3') for *Gapdh* as an internal control. Amplification cycles consisted of 94°C for 4 min, 33 cycles at 94°C for 30 s, at 57°C for 20 s, at 72°C for 30 s, and at 72°C for 7 min for Tg *Sp6* and 94°C for 4 min, 22 cycles at 94°C for 30 s, at 57°C for 30 s, at 72°C for 1 min, and at 72°C for 7 min for *Gapdh*.

Immunohistochemistry

Cranio-facial tissues were isolated and fixed, followed by decalcification as described previously (12). Each incisor segment was embedded in paraffin and a series of longitudinal sections (12-μm thick) were prepared. Samples were immunostained with rabbit anti-rat SP6 antiserum (11) or normal rabbit serum as the primary antibody (1 : 400) using Histofine Simple Stain Rat MAX-PO (R) (Nichirei, Tokyo, Japan). DAB-buffer tablets (Merck, Darmstadt, Germany) were used to visualize the signals. For immunofluorescence, anti-SP6 (11) and goat anti-ferritin light chain (D-18 ; 4 mg/ml ; Santa Cruz Biotechnology, Santa Cruz, CA, USA) were the primary antibodies and Alexa Fluor 594-conjugated chicken anti-rabbit IgG (H+L) and Alexa Fluor 488-conjugated chicken anti-goat IgG (H+L ; 10 mg/ml each ; Molecular Probes, Eugene, OR, USA) were the secondary antibodies.

Histological analysis

The color of incisors from rats was recorded using a digital camera or with an MZ16 stereoscopic microscope (Leica Microsystems, Wetzlar, Germany). At least nine (6 weeks) and four (10 weeks) rats of WT and Tg were examined, respectively. Deparaffinized longitudinal sections of the maxillary incisors were stained with hematoxylin. Ameloblast differentiation was determined using Warshawsky and Smith's classification (1). Images of the longitudinal sections of hematoxylin-stained incisors were captured using a light microscope connected to a CCD camera. The length of the ameloblast layer at each stage was measured using ImageJ software (National Institutes of Health, Bethesda, MD, USA).

Statistical significance was evaluated by unpaired *t*-tests for an indicated data set. Prussian blue staining was performed with 1% potassium ferrocyanide containing 0.5% HCl, followed by counterstaining with Kernechtrot stain solution (Muto Pure Chemicals, Tokyo, Japan) before visualization.

X-ray analysis

Radiographs of Tg rat teeth were obtained using MCT-CB100MF (Hitachi Medico, Tokyo, Japan). The X-ray analysis system was operated at a 50-kV accelerating voltage and a 100-μA probe current.

Measurement of serum iron concentrations

Rat sera were analyzed for non-heme iron concentrations and total iron-binding capacity by SRL Inc. (Tokyo, Japan).

RESULTS

Generation of Sp6 Tg rats

Since *Sp6* expressed not only in ameloblasts, but also in hair follicles and limb buds (13), we chose CMV promoter, which is able to function in many cell-types, to investigate the roles of SP6 in amelogenesis and organogenesis. Before generating *Sp6* Tg rats, we examined whether the Tg vector produced functional SP6 protein by transfecting the vector into the dental epithelial cell line G5 (14). SP6 expression was detected by western blot analysis and its function was confirmed by down-regulation of *follistatin* mRNA level by RT-PCR as shown previously (11). Then, we generated 13 independent founder rats harboring the Tg vector and found enamel discoloration in one line. Judging from quantitative PCR analysis of the line, one copy of Tg construct was integrated into genome (data not shown), and further analyzed this line intensively.

We first examined and observed *Sp6* transgene expression in several Tg rat tissues by transgene-specific RT-PCR (Fig. 1A, B). Transgene was detected in all screened tissue, however, only teeth showed abnormal phenotype. Next SP6 expression and localization was analyzed immunohistochemically using the maxillary incisors from 6-week-old Tg rats (Fig. 1C). SP6 was strongly expressed in the presecretory ameloblasts and contralateral odontoblasts as well as in early secretory ameloblasts in WT and Tg rats. At the maturation proper stage, strong ectopic SP6 expression was uniquely detected in Tg ameloblasts.

Discoloration of incisor enamel in Sp6 Tg rats

Although Tg rats possessed the normal numbers of teeth, the incisors from 6-week-old Tg rats were discolored in contrast to the yellow-colored surface of WT rat incisors (Fig. 2, left). Pigmentation in Tg incisors increased gradually at 10-week-old, but it was still less than that in WT incisors (Fig. 2, right). Discoloration of the incisor enamel in rodents is reminiscent of amelogenesis imperfecta (15, 16) and similar to that in animals fed an iron-deficient diet (17). To understand the reason for incisor discoloration in Tg rats, we examined ameloblast differentiation and enamel formation (Fig. 3A, B). Histological analysis revealed that incisor ameloblasts from WT and Tg rats secreted similar levels of enamel matrices and formed similar Tomes' processes (Fig. 3A) as reported previously (1). X-ray analysis of the maxillae and mandibles from adult rats revealed that the density of thick enamel region was higher than that of the dentin in the incisors and molars from Tg rats (Fig. 3B). These results exclude any type of amelogenesis imperfecta classified by Witkop (18).

Serum iron levels in Tg rats were comparable with those of WT rats (Fig. 3C). Total iron-binding capacity and transferrin saturation levels were similar in both Tg and WT rats (Fig. 3C). These results indicated that Tg rat incisor discoloration was due to neither amelogenesis imperfecta nor serum iron deficiency, but rather perturbed iron transfer from the blood vessels to the enamel surface.

Inhibition of ameloblast differentiation in Tg rats

To investigate the molecular mechanism of discoloration, we examined whether iron transfer was perturbed by ectopic *Sp6* expression. Incisor sections from 6-week-old rats were stained with Prussian blue (Fig. 4A). The iron signals in the incisors of WT rats were strong in the ameloblasts at the pigmentation stage, however, a gradual decrease was observed at the pigment release stage (Fig. 4A). Furthermore, the signal was undetectable at the postpigmentation and reduced stages. In contrast, the signals in ameloblasts from Tg incisor were strong at the pigmentation stage and continued to the gingival margin (Fig. 4A). Hematoxylin-stained section revealed that the yellow pigment remained localized to the same region up to the gingival margin in Tg rats, indicating a delayed appearance of the pigment releases stage (Fig. 4B). Tg rat incisor ameloblasts at the gingival margin retained their
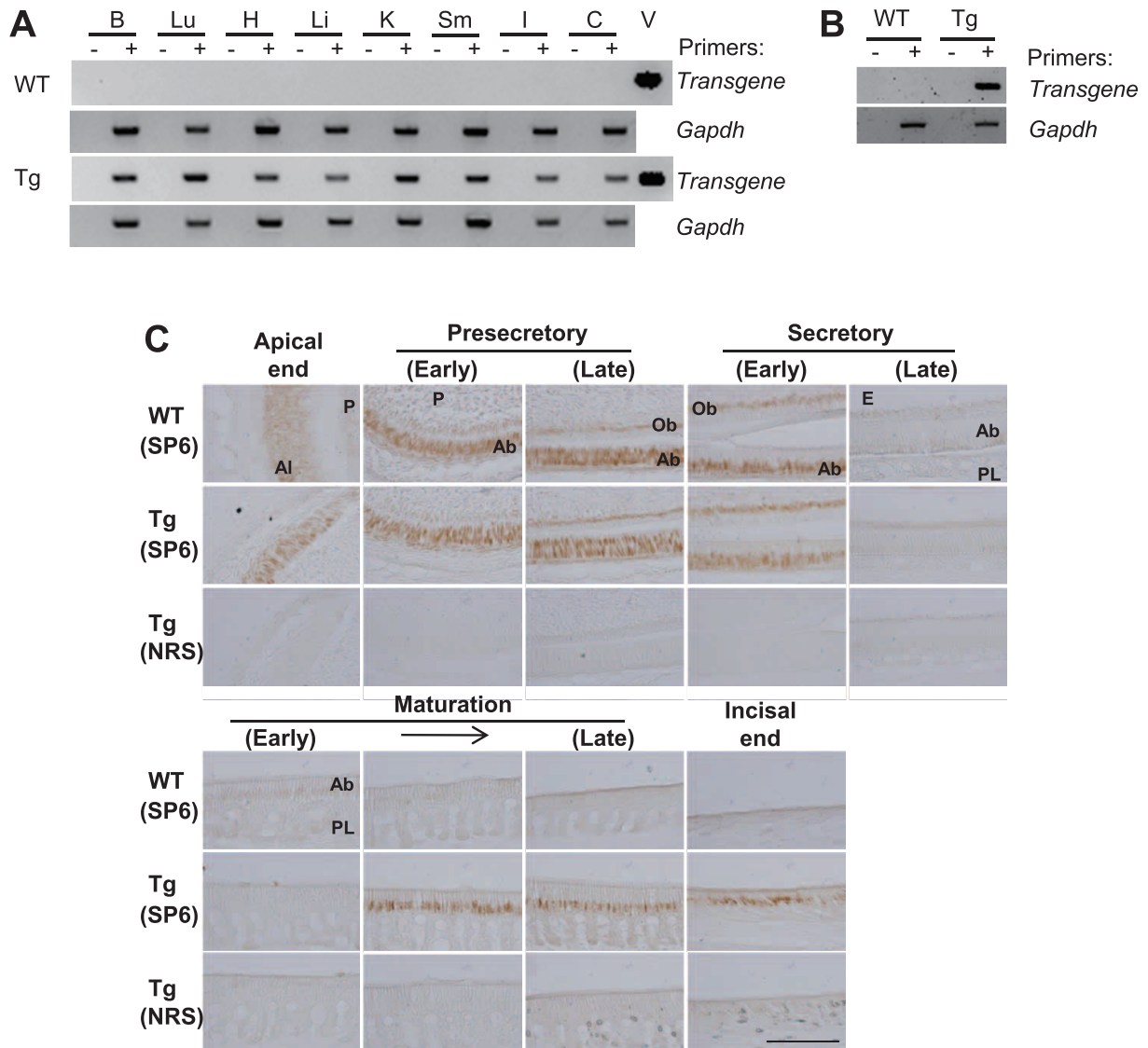
Fig. 1 *Sp6* transgene expression of Tg rat incisors.
(A) *Sp6* transgene expression in various tissues was examined by RT-PCR. B, brain ; Lu, lung ; H, heart ; Li, liver ; K, kidney ; Sm, skeletal muscle ; I, small intestine ; C, colon ; V, plasmid vector containing Tg construct (positive control). "+" and "-" indicate with or without reverse transcriptase, respectively. (B) *Transgene* and *Gapdh* expression was examined in molar tooth germs of WT and Tg pups. "+" and "-" indicate with and without reverse transcriptase, respectively. (C) Sections prepared from maxillary incisor of WT and Tg rats (6wk) were immunostained with antiserum against rat SP6 (SP6) or normal rabbit serum (NRS). Scale bar=100 μm. Ab, ameloblasts ; Al, apical loop ; E, enamel space ; Ob, odontoblasts ; P, pulp ; PL, papillary layer.

columnar shape, whereas WT rat incisor ameloblasts exhibited reduced and contracted morphology (Fig. 4A, B). These results indicate that both iron uptake and storage in Tg rat incisor ameloblasts were intact in ameloblasts, but the iron-releasing step was significantly inhibited or delayed.

The delayed transition from the pigmentation stage to the pigment release stage can be caused either by (i) delayed appearance of the pigmentation stage, (ii) delayed disappearance of it, or (iii) combination of both. To address this question, we measured the length of the ameloblast layer at each differentiation stage using longitudinal incisor sections (Fig. 4C). Length of each layer at the

presecretory, secretory, and sum of the transition and maturation proper stages were similar in WT and Tg rats (Fig. 4C). However, the layer at the pigmentation stage was much longer in incisors from Tg than WT rats, and was not noticeable at the later stages in the incisors from Tg rats (Fig. 4C). Fig. 4D demonstrates the relationship between SP6 expression and ameloblast differentiation stages in WT and Tg rats. Ectopic SP6 expression in Tg rats was observed during the maturation proper and elongated pigmentation stages.

In addition, we found that the lateral edges of the incisors from 6-week-old Tg rats were yellowish (Fig. 2) despite the absence of pigment release
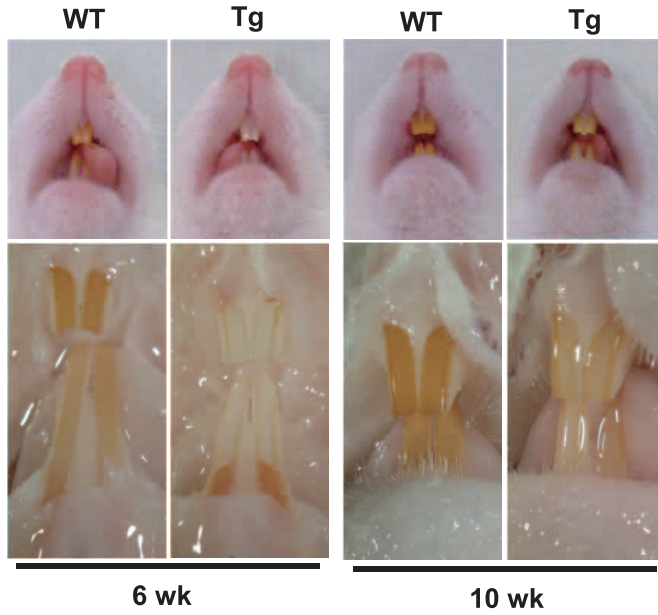
Fig. 2   Discoloration of the incisors from Tg rats.
Representative images of incisors from 6- or 10-week-old WT and Tg rats captured by a digital camera (upper panel) or a stereomicroscope (lower panel) are shown.
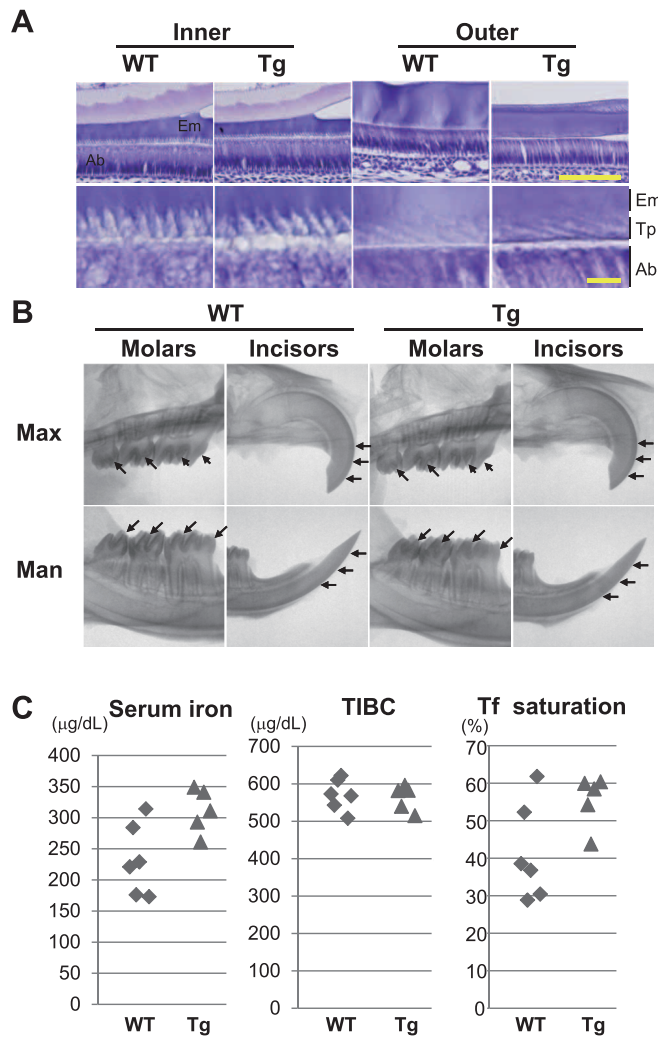

Fig. 3   Amelogenesis and serum iron concentrations from 6-week-old Tg rats. (A) Incisors from WT and Tg rats were histologically examined (Hematoxylin staining). Regions containing the ameloblasts for inner (left) or outer (right) enamel secretion are shown. Scale bar=100 μm (upper panels). High magnification images of Tomes' processes are shown in the lower panels (Scale bar=10 μm). Em, enamel matrix ; Tp, Tomes' processes ; Ab, ameloblasts. (B) Maxillary (Max) or mandibular (Man) molars and incisors from WT and Tg rats are examined by radiography. Arrows indicate radio-opaque enamel formation. (C) Serum iron concentrations, total iron-binding capacity (TIBC), and transferrin (Tf) saturation from 6 WT and 5 Tg rats were analyzed.

(Fig. 4A-D). Examination of the pigment release at the lateral surface of incisors using cross sections revealed that pigment in the ameloblasts at the lateral surfaces was observed in segments 1 and 2 of the incisors from WT rats, while it began to disappear in segment 3 and completely disappeared in segment 4 in a manner similar to that at the labial surfaces (Fig. 4E, F, H). In contrast, in incisors from
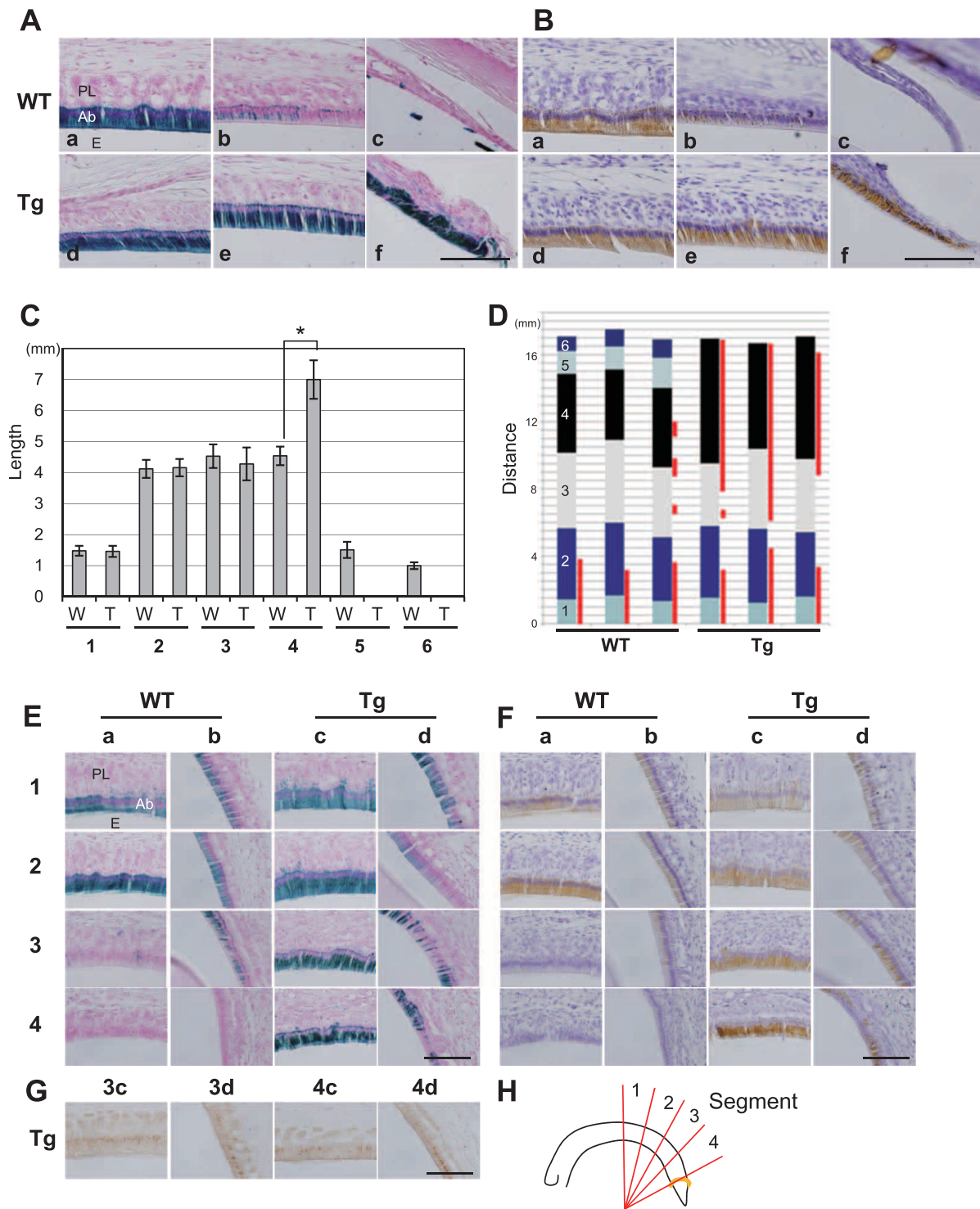
Fig. 4   Perturbed differentiation of incisor ameloblasts from 6-week-old Tg rats.
(A) Prussian blue and (B) hematoxylin staining were performed using longitudinal sections of the maxillary incisors from WT and Tg rats. The pigmentation (a, d), pigment release (b, e), and reduced (c, f) stages in the ameloblast layer of the incisors from WT and Tg rats, respectively, are shown. (C) The length of the ameloblast layer at each differentiation stage in maxillary incisor longitudinal sections was measured. 1, presecretory ; 2, secretory ; 3, transition and maturation proper ; 4, pigmentation ; 5, pigment release and post pigmentation ; and 6, reduced stages. W, WT ; T, Tg. Data represented the average of three independent samples (*P= 0.0034). (D) Ameloblast differentiation stages at a particular length of the trace over the ameloblast layer from the apical end are plotted. Three independent samples of the incisors from WT and Tg rats examined in (C) were analyzed. Red lines beside the column represent the regions in which the ameloblasts express SP6. 1-6, same as in (C). (E-H) Prussian blue staining (E), hematoxylin staining (F), and SP6 immunohistochemistry (G) were performed using coronal sections of maxillary incisors from WT and Tg rats. Ameloblasts at the labial (a, c) and lateral (b, d) surfaces of the incisors are shown. Incisors were cut into segments in the direction of the incisal end as shown in the scheme in (H) for the cross sections. The segment numbers (1-4) in E-G correspond to those in H. Scale bars=100 μm.

Tg rats, the pigment was detected at both the labial and lateral surfaces of all four Tg rat incisor segments, although the pigment was sporadically lost in these locations in segments 3 and 4 (Fig. 4E, F). SP6 signal was detected in Fig. 4G similar to the pigment distribution in the incisor ameloblasts from Tg rats in segment 3 (Fig. 4E, F). SP6-positive cells at both the labial and lateral surfaces decreased near the incisal end of segment 4. Again, we observed the concomitant correlation between SP6 expression and high amount of ameloblast pigment, suggesting

the specific SP6 regulation of maintaining pigments in ameloblasts.

Altered pigment release in Tg rats

We observed that the labial surfaces of the incisors from 10-week-old Tg rats were weakly colored (Fig. 2). Therefore, we examined pigment release from incisor ameloblasts in these rats (Fig. 5). In WT rats, here we used the littermates of Tg rats, the pigment decreased gradually during the pigment-release stage and was not observed in the
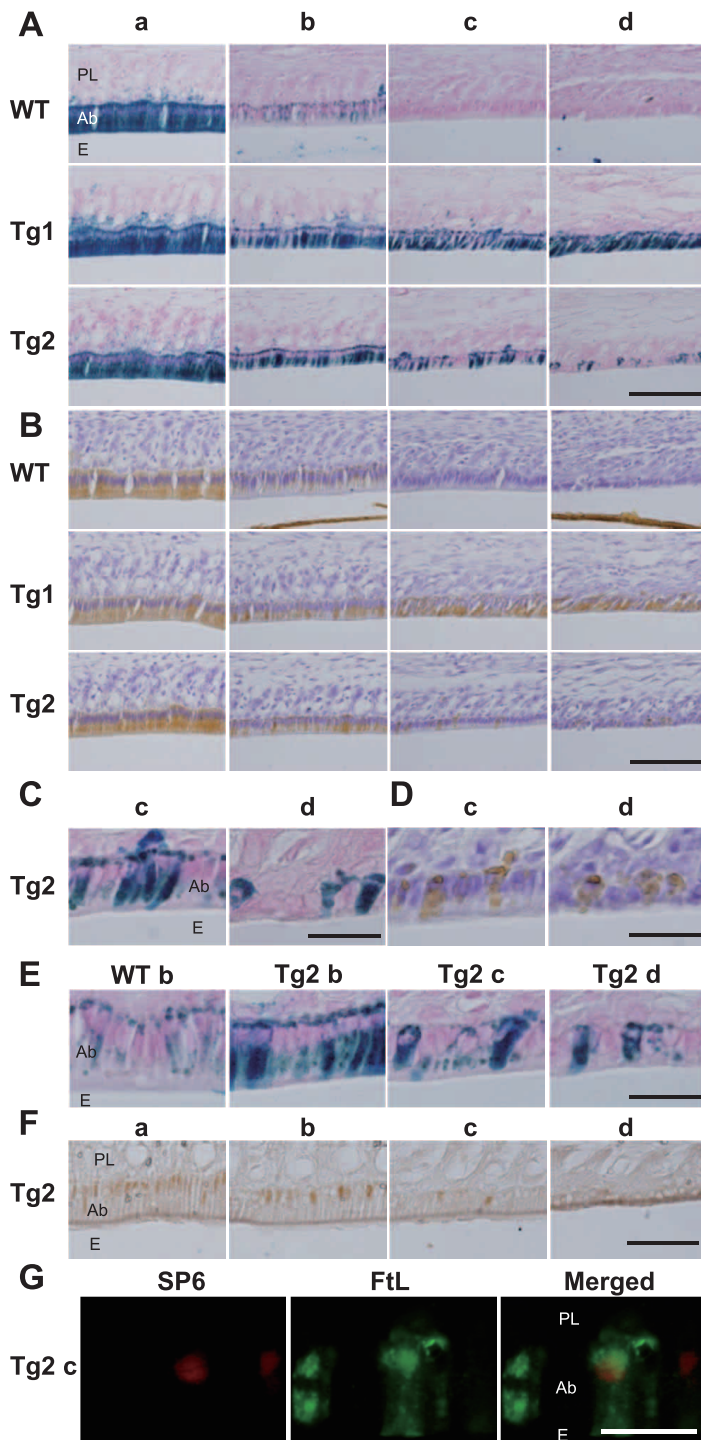

Fig. 5   Perturbed release of pigment from the incisor ameloblasts from 10-week-old Tg rats.
(A-G) Prussian blue staining (A, C, E), hematoxylin staining (B, D), and SP6 immunohistochemistry (F) of ameloblasts were performed using longitudinal sections of the incisor. Double-staining for SP6 (red) and the ferritin light chain (FtL, green) (G) was performed using sections of maxillary incisors from WT and Tg (Tg1, 2) rats. The pigmentation (a), pigment release (b), postpigmentation (c), and reduced (d) stages of the ameloblast layer of incisors from WT and Tg rats were shown. Tg1 and Tg2 were the representative samples with low and high activity for pigment release in the same Tg line. PL, papillary layer ; Ab, ameloblasts ; E, enamel space. Scale bars=100 μm (A, B), 25 μm (C, D, E, G), and 50 μm (F).

postpigmentation and reduced stages (Fig. 5A, B). Interestingly, we found that there were some variations of pigment release in the same Tg line. In some incisors from Tg rats, pigment release was incomplete and sporadic at the pigment release stage, and most of the ameloblasts near the incisal end retained the pigment without ameloblast regression, showing individual differences (Fig. 5A, B, Tg1). In other incisors from Tg rats, pigment release was observed partially at the pigment release stage, and the ameloblasts regressed at the incisal end (Fig. 5A, B, Tg2). Fine examination with higher magnification clearly revealed that the incisor ameloblasts from Tg rats were morphologically similar to those in the postpigmentation and reduced stages from WT rats, but they contained the pigment (Fig. 5C, D). Small pigment granules that represent lysosomal pigment digestion (2, 5) were observed in WT ameloblasts at the pigment release stage. In contrast, such granules in Tg rats, were observed not only in the pigment release stage but also in the postpigmentation and reduced stages (Fig. 5E). SP6 expression in the ameloblasts from Tg rat decreased gradually from the pigmentation to the reduced stage (Fig. 5F), which correlated

with the appearance of sporadic pigment release (Fig. 5A, B).

To examine whether the sporadic SP6 expression in the incisor ameloblasts from Tg rats co-localized with the scattered pigment deposition, the sections were double-stained with antibodies against SP6 and the ferritin light chain, which is believed to be a component of the pigment (2, 5) (Fig. 5G). Some ameloblasts expressed both SP6 and ferritin, whereas others expressed either one or neither (Fig. 5G).

DISCUSSION

Ameloblasts differentiation from the pigmentation to later stages results in pigment loss and a gradual regression of cellular height (1, 2). In this study, we could dissect these concomitant events, iron metabolism and morphological change during amelogenesis through ectopic *Sp6* expression *in vivo*. Our findings are summarized in Fig. 6.

In the incisors of 6-week-old Tg rats, ectopic SP6 expression was detected predominantly in the pigmentation-stage ameloblasts, and specific
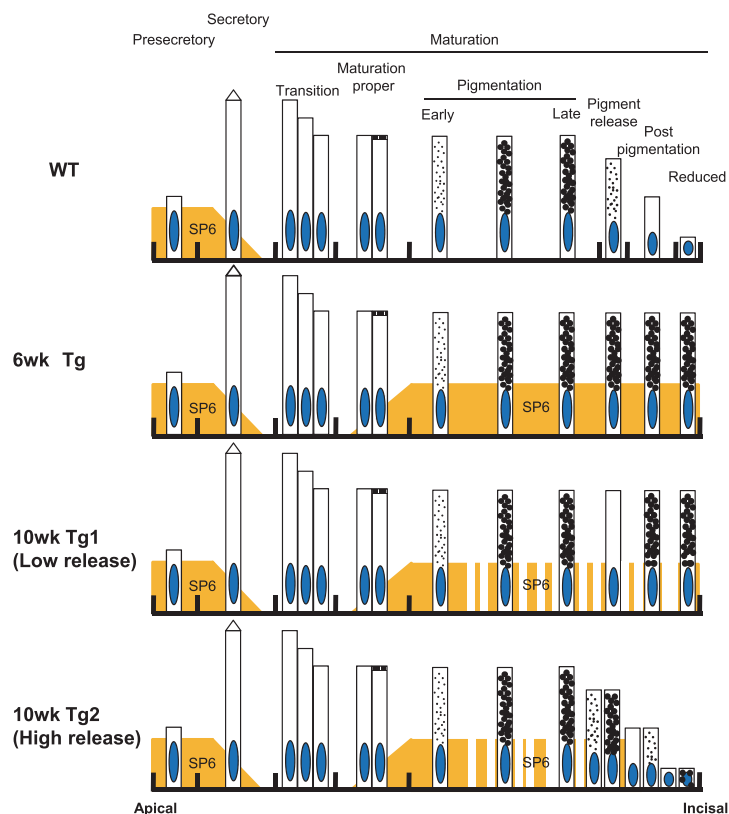

Fig. 6   Summary of the relationship between ameloblast differentiation and SP6 expression in incisors from WT and Tg rats. Ameloblasts at each differentiation stage are shown from the apical bud toward the incisal end. The white squares and blue circles represent the cells and their nuclei, respectively. The black dots and circles indicate the pigment granules in the cells. The yellow bars indicate SP6 localization. Detail explanation is described in the text.

inhibition of pigment removal and cellular shrinkage was observed during this stage (Fig. 4A-D). Ectopic SP6 expression gradually ceased in the ameloblasts near the incisal end in 10-week-old Tg rats, where both the pigment release and the morphologic differentiation of ameloblasts were partially restored (Fig. 5). Concomitantly, ectopic SP6 expression disappeared sporadically in ameloblasts on the lateral surface of the incisors of 6-week-old Tg rats (Fig. 4G), and pigment release of the ameloblasts and staining of the lateral edges of enamel were partially observed (Fig. 2 and Fig. 4E, F). These results indicate that ameloblast differentiation in Tg rats is disturbed through Tg SP6 activity.

In 10-week-old Tg rat incisors, gradual cellular shrinkage was observed along with sporadic SP6 expression in the late maturation-stage ameloblast layer (Fig. 5F). It may indicate that SP6 is not directly involved in inhibiting morphologic differentiation of the ameloblasts. In addition, some ameloblasts in 10-week-old Tg incisors expressed significant amounts of SP6 and negligible amounts of ferritin, whereas others expressed less SP6 and more ferritin (Fig. 5G). These findings demonstrate that SP6 may regulate pigment retention indirectly, because ferritin is a possible pigment constituent, suggesting that another factor or mechanism is involved in this metabolic phase.

We found an expanded ameloblast layer at the pigmentation stage in the longitudinal sections of the incisors from 6-week-old Tg rats (Fig. 6, the second panel). We hypothesized two reasons for it ; disturbed cell number or blocked cell differentiation.

The cell number of ameloblasts is regulated by the balance between proliferation and cell death. Introduction of the *Sp6* transgene may have inhibited ameloblast cell death or activated ameloblast proliferation at the pigmentation stage. Previous studies demonstrated that SP6 has anti-apoptotic (9, 10) and growth-promoting activities (9, 11, 13). Moreover, Smith and Warshawsky reported that 25% of incisor ameloblasts die during the postsecretory transition stage and another 25% die during the later maturation stages (19). However, we could not detect cell death histologically during the later stages in *Sp6* Tg rats (data not shown). Aberrant SP6 expression might disturb the transcriptome and the following metabolome in ameloblasts, resulting in the inhibition of ameloblast differentiation toward the pigment release stage.

In general, ameloblasts in the pigment release stage undergo pigment digestion in WT rat incisors

(Fig. 6, the top panel). Molecular mechanisms regulating pigment release have not been so far established. Two possible mechanisms for the pigment release can be proposed. One is that an internal signal such as cellular stress including excess iron accumulation in the cells may trigger metabolic pathways to exclude the iron-containing pigment. Another is that an external signal surrounding the narrow niche may promote pigment release by the unknown mechanism.

Ameloblasts in the pigment release stage contain small pigment dots through lysosomal pigment digestion (2). Unexpectedly, we observed the pigment digestion in the incisors from 10-week-old Tg rats in the pigment release, postpigmentation, and reduced stages (Fig. 6, the third and fourth panels), although no observation of those stages in 6-weel-old Tg rats. This finding indicated that pigment release itself is under the separate regulation from the presence of Sp6. In addition, some Tg ameloblasts retained pigment until they became much shorter at the postpigmentation and reduced stages (Fig. 6, the fourth panels).

During shrinking of the pigment retaining cells, some of the pigment might be exported gradually from the cells, because the cytoplasmic space filled with in the pigment must be reduced dramatically, indicating that another pigment digestion mechanism could function in the late postpigmentation and reduced stages. Further investigation is necessary to understand the regulatory mechanisms underlying the pigment release and to identify the external signals from the surrounding niche.

Iron metabolism is a critical process for living organisms. Since abnormal accumulation of iron in the cells leads to eventual organ failure via iron-mediated free radical formation (20), tight control of iron metabolism is crucial for survival. Recently, Matak *et al.* reported that *Sp6* orthologs, may be involved in the genetic response to increased intestinal iron absorption (21). It is an interesting issue to determine whether accumulation and metabolism of iron-containing pigment in several organs such as liver, heart, and pancreas is controlled in the same way as pigment retention in the ameloblasts.

In conclusion, *Sp6* Tg rat provides a useful tool to further analyze the new role of SP6 in not only morphological regulation but also iron metabolism in amelogenesis *in vivo*, and suggested temporospatial regulation of SP6 expression is a critical issue to understand amelogenesis.

CONFLICT OF INTEREST

ACKNOWLEDGMENTS

REFERENCES

1. Warshawsky H, Smith CE : Morphological classification of rat incisor ameloblasts. Anat Rec 179 : 423-446, 1974
2. Kallenbach E : Fine structure of rat incisor enamel organ during late pigmentation and regression stages. J Ultrastruct Res 30 : 38-63, 1970
3. Halse A, Selvig KA : Incorporation of iron in rat incisor enamel. Scand J Dent Res 82 : 47-56, 1974
4. Halse A : Location and first appearance of rat incisor pigmentation. Scand J Dent Res 80 : 428-433, 1972
5. Takano Y, Ozawa H : Cytochemical studies on the ferritin-containing vesicles of the rat incisor ameloblasts with special reference to the acid phosphatase activity. Calcif Tissue Int 33 : 51-55, 1981
6. Selvig KA, Halse A : The ultrastructural localization of iron in rat incisor enamel. Scand J Dent Res 83 : 88-95, 1975
7. Suske G, Bruford E, Philipsen S : Mammalian SP/KLF transcription factors : bring in the family. Genomics 85 : 551-556, 2005
8. Talamillo A, Delgado I, Nakamura T, de-Vega S, Yoshitomi Y, Unda F, Birchmeier W, Yamada Y, Ros MA : Role of Epiprofin, a zinc-finger transcription factor, in limb development. Dev Biol 337 : 363-374, 2010
9. Nakamura T, de Vega S, Fukumoto S, Jimenez L, Unda F, Yamada Y : Transcription factor epiprofin is essential for tooth morphogenesis by regulating epithelial cell fate and tooth number. J Biol Chem 283 : 4825-4833, 2008
10. Hertveldt V, Louryan S, van Reeth T, Dreze P, van Vooren P, Szpirer J, Szpirer C : The development of several organs and appendages is impaired in mice lacking Sp6. Dev Dyn 237 : 883-892, 2008
11. Ruspita I, Miyoshi K, Muto T, Abe K, Horiguchi T, Noma T : Sp6 downregulation of follistatin gene expression in ameloblasts. J Med Invest 55 : 87-98, 2008
12. Smith CE : A method for preparing longitudinal semi-thin Epon sections of entire rat incisors. Arch Oral Biol 19 : 1045-1048, 1974
13. Nakamura T, Unda F, de-Vega S, Vilaxa A, Fukumoto S, Yamada KM, Yamada Y : The Kruppel-like factor epiprofin is expressed by epithelium of developing teeth, hair follicles, and limb buds and promotes cell proliferation. J Biol Chem 279 : 626-634, 2004
14. Abe K, Miyoshi K, Muto T, Ruspita I, Horiguchi T, Nagata T, Noma T : Establishment and characterization of rat dental epithelial derived ameloblast-lineage clones. J Biosci Bioeng 103 : 479-485, 2007
15. Asaka T, Akiyama M, Domon T, Nishie W, Natsuga K, Fujita Y, Abe R, Kitagawa Y, Shimizu H : Type XVII collagen is a key player in tooth enamel formation. Am J Pathol 174 : 91-100, 2009
16. Miskin R, Masos T, Shoham Z, Williams-Simons L : Urokinase-type plasminogen activator mRNA is expressed in normal developing teeth and leads to abnormal incisor enamel in alpha MUPA transgenic mice. Transgenic Res 15 : 241-254, 2006
17. Halse A : Effect of dietary iron deficiency on the pigmentation and iron content of rat incisor enamel. Scand J Dent Res 81 : 319-334, 1973
18. Witkop CJ, Jr. : Amelogenesis imperfecta, dentinogenesis imperfecta and dentin dysplasia revisited : problems in classification. J Oral Pathol 17 : 547-553, 1988
19. Smith CE, Warshawsky H : Quantitative analysis of cell turnover in the enamel organ of the rat incisor. Evidence for ameloblast death immediately after enamel matrix secretion. Anat Rec 187 : 63-98, 1977
20. Andrews NC, Schmidt PJ : Iron homeostasis. Annu Rev Physiol 69 : 69-85, 2007
21. Matak P, Deschemin JC, Peyssonnaux C, Vaulont S : Lack of iron-related phenotype in Sp6 intestinal knockout mice. Blood Cells Mol Dis 47 : 46-49, 2011